

Spectroscopic Studies of Phosphazene Polymers Containing Photoluminescent Metal Complexes

Eric W. Ainscough,^{*[a]} Harry R. Allcock,^[b] Andrew M. Brodie,^{*[a]} Keith C. Gordon,^{*[c]}
Mark D. Hindenlang,^[b] Raphael Horvath,^[c] and Carl A. Otter^[a]

Keywords: Phosphazenes / Polymers / Rhenium / Palladium / Platinum

A series of small phosphazene ligands with pendant 6-phenyl-2,2'-bipyridyl moieties, namely L¹ [N₃P₃(OPh)₅(OPhbpPh)], L² [N₃P₃(biph)₂(OPhbpPh)₂], L³ [N₃P₃(*t*Bu-biph)₂(OPhbpPh)₂], L⁴ [N₃P₃(biph)₂(OPhbpPh)Cl] and L⁵ [N₃P₃(biph)₂(OPhbpPh)(OPh)] [OPhbpPh = 4-(4-phenoxy)-6-phenyl-2,2'-bipyridine, OPh = phenoxy, biph = 2,2'-oxybiphenyl and *t*Bubiph = 4,4'-di-*tert*-butyl-2,2'-oxybiphenyl], have been used to synthesise the new cyclometallated palladium(II) and platinum(II) complexes [(L¹-H)PdCl], [(L¹-H)-PtCl], [(L¹-H)(PdCl)₂], [(L³-H)(PdCl)₂], [(L⁴-H)PtCl], [(L⁵-H)-PtCl] and the rhenium(I) complex [L⁵Re(CO)₃Cl]. Single-crystal X-ray diffraction analysis was performed on the free ligand L² and the palladium complexes [(L¹-H)PdCl] and [(L³-H)(PdCl)₂]. In both Pd^{II} complexes, the metal centre lies in a distorted square-planar geometry with an "N₂CCl" do-

nor set confirming the cyclopalladation. The ligand pendant arms are involved in intermolecular stacking interactions with adjacent molecules. A polyphosphazene (L⁶) with 4-*tert*-butylphenoxy (*Ot*BuPh) and the potential donor OPhbpPh as pendant groups was prepared and used to synthesise metallopolymers with Re^I and Pt^{II}. Spectroscopic and computational studies were conducted to compare the discrete complexes with the polymers with similar metal pendants as well as to model compounds in the literature. By using UV/Vis and resonance Raman spectroscopic techniques it was found that very few deviations from known metal chromophores exist for both the triphosphazene- and polyphosphazene-based complexes. The transient resonance Raman spectra of the Pt^{II} complexes revealed a ligand radical anion signature associated with the N₂C unit.

Introduction

The synthesis of new polymers containing transition-metal complexes is an area of research that is attracting increasing interest^[1–3] due to a diverse range of prospective applications for polymer-based metal complexes, including sensors,^[4–7] biomedical applications^[8–10] and catalysis.^[11,12] Owing to their well-understood emissive properties,^[13] metal complexes have attracted attention in the field of organic light-emitting diode (OLED) device construction^[14] and examples of electroluminescent polymers containing metal ions as chromophores are also becoming more widespread.^[15–17] One aspect that is of significance for OLED

design is the fact that the photophysical properties of the chromophores can be tuned by using substituents on the polymer support.^[18–20]

Phosphazene systems are good candidates for such applications as the polymer backbone can be easily derivatised, allowing the development of a wide range of polymers containing various ligands and metal complexes.^[21] The influence of different substituents on the physical properties of a polymer, such as the glass transition temperature (*T*_g), is also well understood.^[22] Hence, the systematic design of a luminescent material with the desired properties for fabrication of a specific device should be achievable. Indeed, the possibility of adapting cyclic and polymeric phosphazenes to this end has been proposed in several earlier reports.^[23–28]

Recently we reported the preparation and excited-state spectroscopic studies of a series of cyclic phosphazenes containing Ru^{II} and Re^I bipyridine complexes and found that there is little interaction between the phosphazene core and the chromophore.^[29] We have now extended the study to examine the photophysical properties of polymeric Re^I and Pt^{II} derivatives as well as related small-molecule compounds. We report herein the synthesis and spectroscopy of the new systems and also describe the crystallography of two new Pd^{II}-containing cyclic analogues.

[a] Chemistry-Institute of Fundamental Sciences, Massey University, Private Bag 11 222, Palmerston North 4442, New Zealand
Fax: +64-6-3505602
E-mail: e.ainsoug@massey.ac.nz
a.brodie@massey.ac.nz

[b] Department of Chemistry, The Pennsylvania State University, University Park, PA 16802, USA

[c] MacDiarmid Institute for Advanced Materials and Nanotechnology, Department of Chemistry, University of Otago, Dunedin 9054, New Zealand
Fax: +64-3-4797906
E-mail: kgordon@chemistry.otago.ac.nz

Supporting information for this article is available on the WWW under <http://dx.doi.org/10.1002/ejic.201100341>.

Results and Discussion

Small-Molecule Compounds: Synthesis of Ligands and Complexes

The ligand L^1 (Figure 1) was prepared by the reaction of HOPhbpPh with the phosphazene $N_3P_3(OPh)_5Cl$ as described previously.^[29] Similarly, the new phosphazenes L^2 , L^3 and L^4 were prepared by the reaction of 1 or 2 equiv. of the sodium salt of HOPhbpPh with $N_3P_3(biph)_2Cl_2$ or $N_3P_3(tBubiph)_2Cl_2$ in the presence of the catalyst, tetrabutylammonium bromide (Scheme 1). The ^{31}P NMR spectra of L^2 and L^3 both contain the anticipated two-phosphorus doublet and one-phosphorus triplet resonances (see the Exp. Sect.). During the preparation of L^2 we observed the appearance of a singlet at $\delta = 22.70$ ppm corresponding to the monosubstituted species L^4 . This phosphazene can be prepared from the reaction between 1 equiv. of the sodium salt of HOPhbpPh with a slight excess of $N_3P_3(biph)_2Cl_2$ and isolated by chromatography. It can then be used as a starting material for further substitution reactions; hence L^5 was prepared from the subsequent reaction of L^4 with sodium phenolate.

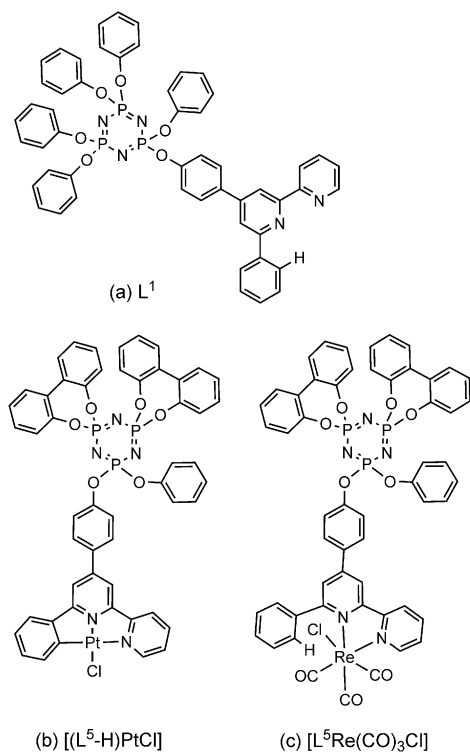


Figure 1. (a) Ligand L^1 (ref.^[29]). (b,c) Representative examples of metal complexes.

Representative examples of the metal complexes are depicted in Figure 1. Organopalladium complexes were prepared from L^1 , L^2 and L^3 by reaction of the ligands with $[Pd(PhCN)_2Cl_2]$ in methanol/benzene at reflux to give cyclometallated 6-phenyl-2,2'-bipyridine complexes with the same " N_2CCl " coordination environment of the metal as in

$[(L-H)PdCl]$ ($L = HOPhbpPh$),^[30] for example, $[(L^1-H)PdCl]$. The disubstituted ligands L^2 and L^3 afforded the di-metallic complexes $[(L^2-H)\{PdCl\}_2]$ and $[(L^3-H)\{PdCl\}_2]$, which precipitated directly from the mother liquor. Recrystallisation from dimethyl sulfoxide (DMSO) gave compounds that retained solvated DMSO and showed negligible solubility in common organic solvents other than dimethylformamide (DMF). The crystals of $[(L^2-H)\{PdCl\}_2]$ that initially form gave microanalytical data consistent with the presence of three DMSO solvate molecules after drying under vacuum overnight. Drying under vacuum for another 48 h removed two of these molecules and the final DMSO was removed by heating the complex under vacuum at 75 °C.

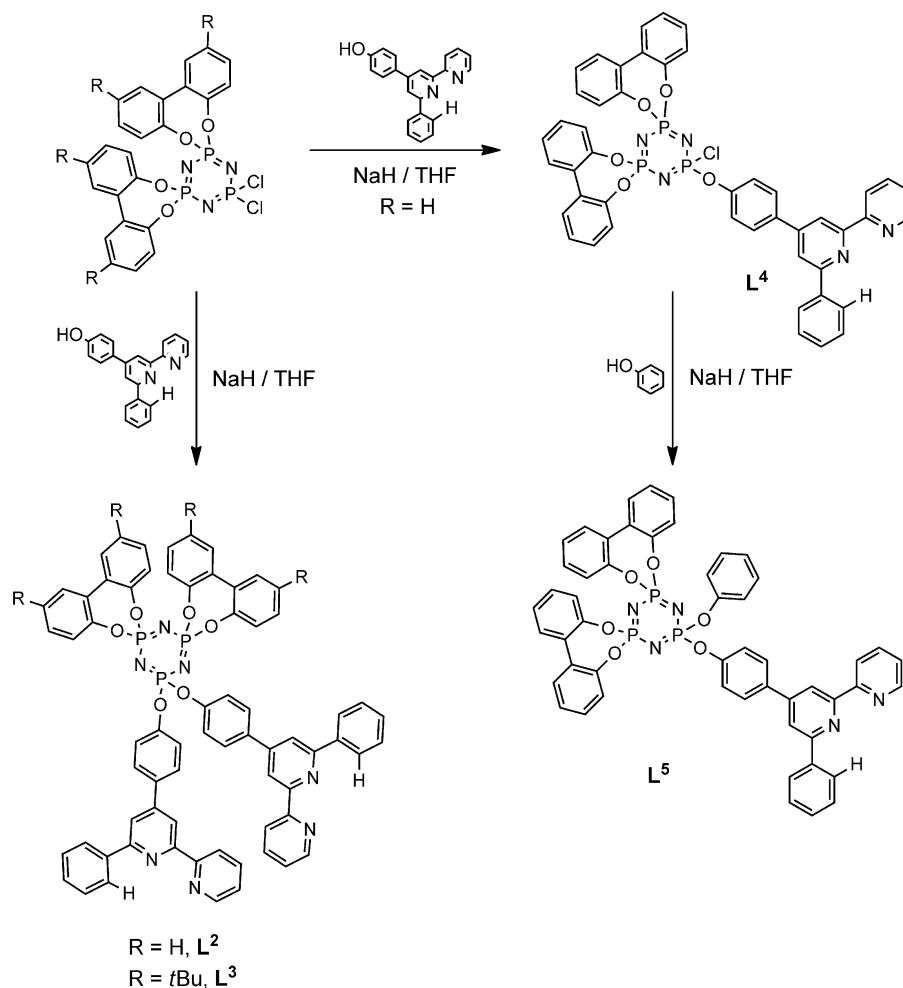
The complex $[(L^3-H)\{PdCl\}_2]$ is only marginally more soluble than $[(L^2-H)\{PdCl\}_2]$ in DMSO, which is surprising because other *tBubiph*-substituted phosphazenes are highly soluble. Crystals of $[(L^3-H)\{PdCl\}_2]$ suitable for X-ray analysis were obtained by recrystallisation by vapour diffusion of EtOH into a DMF solution of the complex. The data only refined well when the contributions from disordered solvent molecules (both DMF and EtOH, corresponding to 1278 electrons per molecule of the complex) were removed from the model. Complexes $[(L^1-H)PdCl]$ and $[(L^4-H)PdCl]$ are readily soluble in CH_2Cl_2 or $CHCl_3$, which suggests that the lack of solubility of $[(L^2-H)\{PdCl\}_2]$ and $[(L^3-H)\{PdCl\}_2]$ is due to extensive intermolecular stacking networks, which are possible as a result of the two flat, cyclometallated aromatic ligand arms (see the Crystal Structures section). These motifs are common in planar Pd^{II} and Pt^{II} complexes of polypyridine ligands.

Organoplatinum complexes of L^1-H and L^5-H were prepared in a similar manner to the organopalladium complexes starting from $[Pt(PhCN)_2Cl_2]$. However, the double cycloplatination of L^2 and L^3 did not occur as readily as the corresponding double cyclopalladation and we did not obtain samples free of the monoplating product. From the reaction between $N_3P_3(biph)_2Cl_2$ and 1 equiv. of $[(L-H)PtCl]$ ($L = HOPhbpPh$)^[7] in the presence of Cs_2CO_3 as base, we were able to obtain the complex $[(L^4-H)PtCl]$. When 2 equiv. of $[(L-H)PtCl]$ were used in a similar reaction with $N_3P_3(tBubiph)_2Cl_2$, the product $[(L^3-H)\{PtCl\}_2]$ was obtained but, as with the double cycloplatination reactions, a satisfactory separation from the small amount of monosubstituted material present in the reaction mixture was not achieved. The reaction of L^5 with $[Re(CO)_5Cl]$ produced the complex $[L^5Re(CO)_3Cl]$ (Figure 1, c) in which the phosphazene acts as a bidentate ligand through the nitrogen atoms of the bipyridyl unit.

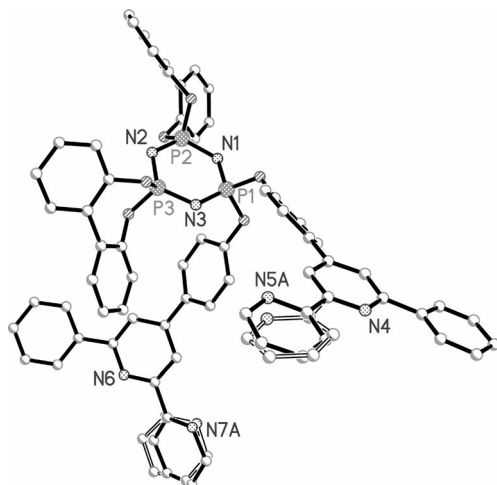
Crystal Structures

 $L^2 \cdot CH_2Cl_2$

Crystals of the ligand L^2 were grown from CH_2Cl_2 /hexane solution and the structure (Figure 2 and Table 1) confirms the double substitution of the biphenyl-derived precursor phosphazene with ligand moieties. The phosphazene

Scheme 1. Synthesis of the cyclotriphosphazene ligands L^2 , L^3 , L^4 and L^5 .

ring is essentially planar with the P–N bond lengths [1.576(3) to 1.582(3) Å] and angles (PNP average 121.6° and NPN average 118.1°) being typical for cyclotriphosphazenes.^[22]

Figure 2. Crystal structure of L^2 .Table 1. Selected bond lengths [Å] and angles [°] for L^2 .

P1–N1	1.581(3)	P2–N2	1.577(3)
P1–N3	1.579(3)	P3–N2	1.582(3)
P2–N1	1.579(3)	P3–N3	1.575(3)
N1–P1–N3	117.79(17)	P1–N1–P2	121.40(19)
N3–P3–N2	118.09(16)	P2–N2–P3	121.3(2)
N2–P2–N1	118.40(16)	P3–N3–P1	121.9(2)

Both ligand arms in the structure are involved in offset π -stacking interactions with the ligand arms of adjacent molecules. These interactions and other H– π and π – π arrays are prominent in the crystal packing and channels containing disordered solvent molecules are formed in the lattice in a way similar to that seen in other substituted cyclic phosphazenes with a high aromatic content.^[29,31–36]

$[(\text{L}^1\text{-H})\text{PdCl}]$

Yellow needles of the complex $[(\text{L}^1\text{-H})\text{PdCl}]$ were grown by the slow diffusion of CH_3OH into a CH_2Cl_2 solution of the complex. The crystal structure (Figure 3a and Table 2)

confirms the cyclopalladation of the phosphazene ligand. The Pd^{II} centre lies in a distorted square-planar geometry with an “N₂CCl” donor set.

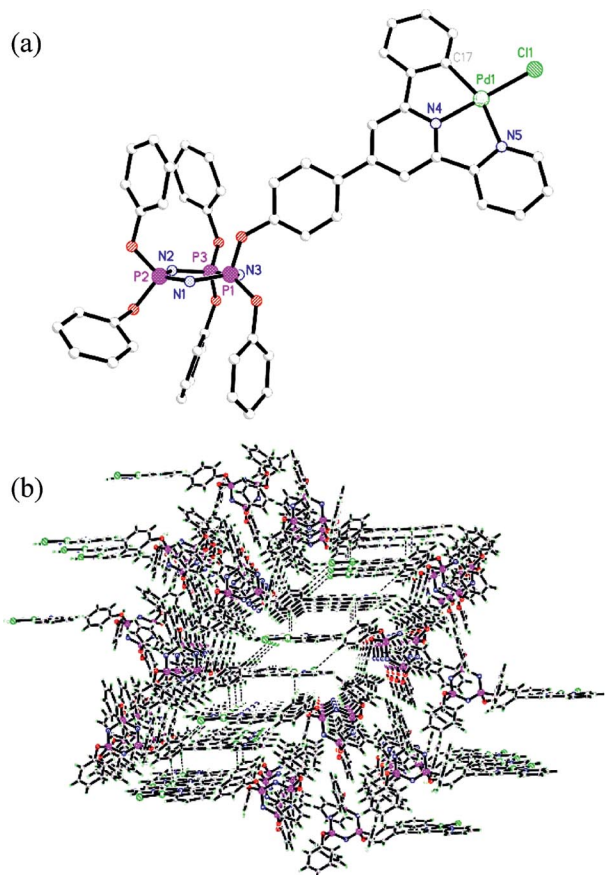


Figure 3. (a) Crystal structure of [(L¹-H)PdCl]. (b) Intermolecular packing in the compound showing extended π -stacking.

Table 2. Selected bond lengths [Å] and angles [°] for [(L¹-H)PdCl].

Pd1–C17	2.062(4)	Pd1–N5	2.087(4)
Pd1–N4	1.963(3)	Pd1–Cl1	2.3164(11)
P1–N1	1.582(3)	P2–N2	1.572(3)
P1–N3	1.575(3)	P3–N2	1.587(3)
P2–N1	1.588(3)	P3–N3	1.591(3)
N4–Pd1–C17	80.42(15)	N5–Pd1–Cl1	99.82(10)
N4–Pd1–N5	79.90(14)	N4–Pd1–Cl1	177.86(10)
C17–Pd1–Cl1	99.93(11)	C17–Pd1–N5	160.17(14)
N1–P1–N3	117.84(18)	P1–N1–P2	120.6(2)
N1–P2–N2	117.37(18)	P1–N3–P3	121.7(2)
N2–P3–N3	116.42(18)	P2–N2–P3	123.1(2)

The Pd–N and Pd–C bond lengths in the terminal aromatic rings of the ligand are similar at 2.087(4) and 2.062(4) Å, respectively. The length of the Pd–N bond to the central pyridine ring is slightly shorter at 1.963(3) Å and the Pd–Cl distance is 2.3164(11) Å. The geometric parameters about the metal centre are very similar to those reported for the complex [Pd(Phbpy)Cl] (Phbpy = 6-phenyl-2,2'-bipyridine).^[37] The P–N distances in the phosphazene

ring are similar [between 1.572(3) and 1.591(3) Å] and the PNP (average 121.8°) and NPN (average 117.2°) angles are also typical.^[22] For comparison, selected calculated bond lengths and angles are shown in Table S1.

The ligand plane is involved in offset π -stacking interactions with the ligand planes of adjacent molecules in the crystal giving rise to staggered layers of the complex moieties running approximately along the *a* axis (Figure 3, b). The molecules are arranged in a “pair-wise” manner so that the origins of the stacking interactions differ on either side of the coordinated ligand plane. On one face, the ligand arms approach so that the Pd^{II} centre lies approximately 3.412 Å from C19 of the coordinated phenyl ligand of the adjacent molecule and the chloride ligands hydrogen bond to H5 of the 4-phenoxy spacer groups in a symmetrical array (Figure 3, b). On the other side of the ligand plane, the rings are offset so that the central pyridine ring lies close to a terminal ligand ring on the adjacent molecule requiring the Pd^{II}–Pd^{II} separation to be larger between these faces (7.034 Å, cf. 5.037 Å).

[(L³-H)(PdCl)₂]

Yellow plates of [(L³-H)(PdCl)₂] were grown from the diffusion of ethanol vapour into a DMF solution of the complex. The crystal structure (Figure 4a) confirms the double cyclometallation of L³ and selected bond lengths and angles are given in Table 3.

Table 3. Selected bond lengths [Å] and angles [°] for [(L³-H)(PdCl)₂].

Pd1–N4	1.958(4)	Pd2–N6	1.975(4)
Pd1–N5	2.139(5)	Pd2–N7	2.092(5)
Pd1–C18	1.988(6)	Pd2–C40	2.059(5)
Pd1–Cl1	2.3093(15)	Pd2–Cl2	2.3165(16)
P1–N1	1.575(5)	P2–N2	1.569(5)
P1–N3	1.574(5)	P3–N2	1.582(5)
P2–N1	1.570(5)	P3–N3	1.593(5)
N4–Pd1–C18	80.8(2)	N6–Pd2–C40	80.2(2)
N4–Pd1–N5	79.42(17)	N6–Pd2–N7	79.95(8)
N5–Pd1–Cl1	100.58(12)	N7–Pd2–Cl2	98.25(14)
C18–Pd1–Cl1	99.14(17)	C40–Pd2–Cl2	101.67(16)
C18–Pd1–N5	160.2(2)	C40–Pd2–N7	160.1(2)
N4–Pd1–Cl1	176.02(12)	N6–Pd2–Cl2	177.32(13)
N1–P2–N2	118.1(3)	P1–N1–P2	123.2(3)
N1–P1–N3	116.9(3)	P1–N3–P3	121.7(3)
N2–P3–N3	117.9(3)	P2–N2–P3	121.5(3)

The two Pd^{II} coordination environments are distorted square planes and comparable to that in [(L¹-H)PdCl]. However, the two sites are not identical: Pd2 has similar Pd–C and Pd–N bond lengths in the terminal bonding rings of the ligand arms [2.060(6) and 2.090(5) Å, respectively], whereas Pd1 has a long Pd–N [2.142(5) Å] and short Pd–C [1.984(6) Å] distance.

The ligand arms on the molecule are orientated such that they extend in opposite directions above and below the plane of the phosphazene ring. Both ligand arms are involved in intermolecular stacking interactions with adjacent

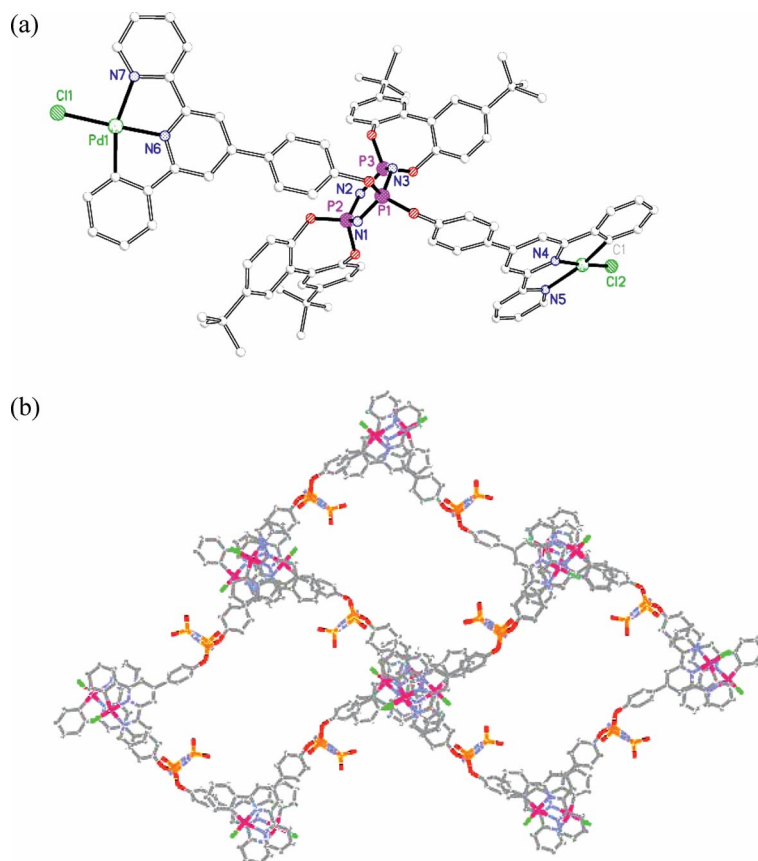


Figure 4. (a) Crystal structure of $[(L^3\text{-H})(\text{PdCl})_2]$. (b) Representation of the long-range packing motif in $[(L^3\text{-H})(\text{PdCl})_2]$ showing the formation of rectangular channels (2,2'-oxybiphenyl groups that occupy the channels have been excluded for clarity).

molecules, as observed with $[(L^1\text{-H})\text{PdCl}]$ and similar complexes. However, the presence of two planar aromatic arms pointing in opposite directions gives rise to an interesting long-range motif. The metal centres are stacked along the c axis at the corners of an interlocking rectangular array in which one molecule spans two corners to form one side of the rectangle (Figure 4, b). The resulting grids contain large channels containing disordered solvent and the structure only refined well when the contributions made by the solvent molecules to the diffraction data were removed. A large void comprising approximately 30% of the total crystal volume was left after this treatment. This feature of the solid-state structure could explain the poor solubility of the complex and its retention of solvent.

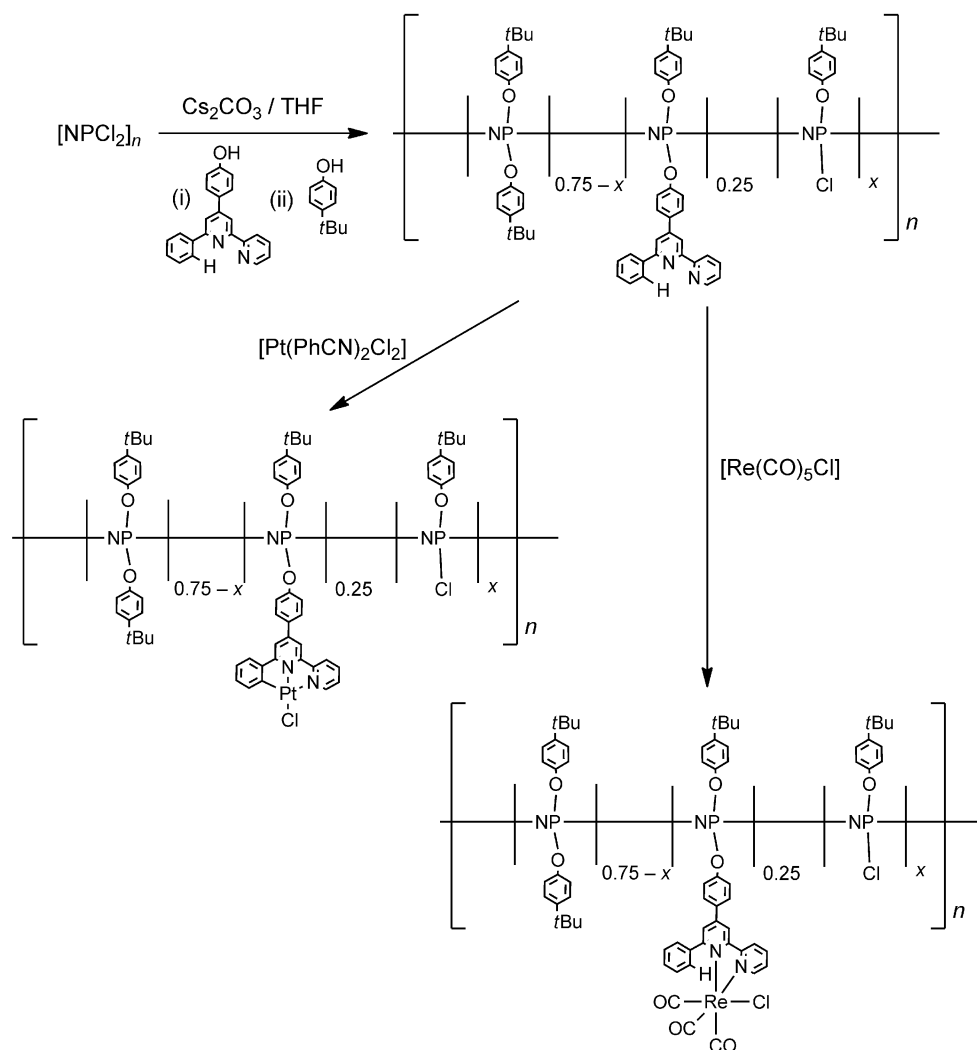
Synthesis and Characterisation of Polyphosphazenes

We initially tried to produce phosphazene copolymers containing OPhbpyPh and trifluoroethoxy (TFE) pendant groups from sequential reactions of the corresponding sodium salts with $(\text{NPCl}_2)_n$. The substitution of Na-OPhbpyPh on the polymer backbone is rapid [the sodium salt of OPhbpyPh is yellow in solution and the colouration disappears almost instantly when added to a solution of $(\text{NPCl}_2)_n$ at room temperature]. However, complete substitution of the TFE groups was only achieved when an excess

of TFE was added and this had the unwanted side-effect of replacing some of the OPhbpyPh moieties with TFE (with recurrence of the yellow colouration in the reaction mixture). Hence we obtained polymers with lower OPhbpyPh content than expected (around 7%). Furthermore, metal complexes of these polymers showed poor solubility after work-up so we examined a different system.

When the sodium salt of 4-*tert*-butylphenol (*t*BuPhOH) was added to the reaction mixture instead of TFE, substitution occurred without replacement of OPhbpyPh, but we could not achieve complete substitution of the chloro groups. Hence, by using a large excess of *t*BuPhOH in the presence of the promoter tetrabutylammonium bromide (TBAB) over extended reaction times and a higher boiling solvent such as toluene, the best result was a polymer formulated as $\{[\text{NP}(\text{O}t\text{BuPh})_2]_{0.5}[\text{NP}(\text{OPhbpyPh})(\text{O}t\text{BuPh})]_{0.25}[\text{NP}(\text{O}t\text{BuPh})\text{Cl}]_{0.25}\}_n$. The difficulties associated with this process are consistent with reports in the literature,^[22] although fully substituted $[\text{NP}(\text{O}t\text{BuPh})_2]_n$ can be obtained.^[38] Interestingly, even though 25% of the polymeric units contained unreacted P–Cl units, the polymer was subjected to work-up under aqueous conditions and showed no signs of hydrolysis or cross-linking.

The maximum replacement of P–Cl units was achieved by first treating $(\text{NPCl}_2)_n$ with 0.25 molequiv. of HOPhbpyPh in the presence of Cs_2CO_3 in THF to produce



Scheme 2. Syntheses of the polyphosphazene L^6 and metallo-polymers.

$\{[NP(OPhbpyPh)Cl]_{0.25}[NPCl_2]_{0.75}\}_n$ (Scheme 2). Subsequent addition of an excess of *t*BuPhOH and reaction for 7 days at reflux in the presence of TBAB resulted in polymers containing between 4 and 8% $[NP(OtBuPh)Cl]$ units, for example, $\{[NP(OtBuPh)_2]_{0.75-x}[NP(OtBuPh)(OPhbpyPh)]_{0.25}[NP(OtBuPh)Cl]_x\}_n$ ($x = 0.06$), designated as L^6 . These polymers were also stable to aqueous work-up and showed no signs of decomposition after several months. Stable polyphosphazenes that contain unreacted chlorine atoms have been reported previously in systems with sterically hindering side-groups.^[38–40] That the residual P–Cl units fail to remain unsubstituted and resistant to hydrolysis is probably because they are so sterically protected by hydrophobic groups that neither aryl oxide ions nor water molecules can reach them.

The reaction of L^6 with $[Pt(PhCN)_2Cl_2]$ in a 1:1 mixture of THF and toluene at reflux produced the orange, cycloplatinated polymer $[L^6\{PtCl\}_{0.25}]_n$, which, after washing with EtOH and drying under vacuum, remained soluble in THF and $CHCl_3$ and partially soluble in CH_2Cl_2 . The reaction of L^6 with $[Re(CO)_5Cl]$ in THF at reflux yielded the

yellow polymer $[L^6\{Re(CO)_3Cl\}_{0.25}]$. This polymer is soluble in $CHCl_3$ and CH_2Cl_2 after washing with EtOH and drying but does not redissolve in THF. The characterisation data of the new polymers are given in the Exptl. Sect. The increase in the polydispersity index (PDI) from 1.97 for the metal-free polymer L^6 to over 2 on addition of Pt or Re is consistent with some thermal degradation of the backbone chain. The increase in the glass transition temperature (T_g) from 83 °C for L^6 to 120 °C for $[L^6\{Re(CO)_3Cl\}_{0.25}]$ suggests the carbonyl ligands bound to the Re interact with the hydrogen atoms from the pendant *Ot*BuPh groups. Similar weak C–H⋯O interactions involving CO ligands have been observed in small-molecule complexes.^[41,42] Interactions similar to the intermolecular π -stacking of the pendant arms seen in the small molecules L^2 and $[(L^3-H)(PdCl)_2]$ are unlikely in the polymers because the pendant arms are probably spaced well apart from each other. The phosphorus NMR spectroscopic data for the polyphosphazenes all show resonances at about –18 ppm, which can be assigned to the phosphorus atoms bound to the *Ot*BuPh and *O*PhbpyPh groups and can be compared with the value of

–17.1 ppm observed for the fully substituted polymer $[\text{NP}(\text{O}t\text{BuPh})_2]_n$.^[38] The metal-free polymer L^6 also shows a broad, poorly resolved shoulder at around –19 ppm, indicative of the presence of chlorine atoms bound to the phosphorus backbone, as in $\text{P}(\text{O}t\text{BuPh})\text{Cl}$ units. The Re^{I} and Pt^{II} polymers exhibit a similar feature although it is not as well resolved. The results of other spectroscopic studies (see below) are consistent with $[\text{L}^6\{\text{Re}(\text{CO})_3\text{Cl}\}_{0.25}]$ and $[\text{L}^6(\text{PtCl})_{0.25}]_n$ having the same coordination environments as their small-molecule analogues.

Spectroscopic Analysis

A variety of spectroscopic studies were performed on the small-molecule complexes $[(\text{L}^1\text{-H})\text{PtCl}]$, $[(\text{L}^1\text{-H})\text{PdCl}]$, $[(\text{L}^4\text{-H})\text{PtCl}]$, $[\text{L}^5\text{Re}(\text{CO})_3\text{Cl}]$ and $[(\text{L}^5\text{-H})\text{PtCl}]$ as well as on the polymers $[\text{L}^6\{\text{Re}(\text{CO})_3\text{Cl}\}_{0.25}]$ and $[(\text{L}^6\text{-H})(\text{PtCl})_{0.25}]$. Density functional theory (DFT) calculations were performed on the small-molecule complexes as well as related model chromophores to aid the description of experimental observations. The effectiveness of the computational calculations was gauged by comparison of a number of calculated and experimental properties.^[43,44] A robust method used to determine if the calculation is modelling the molecule effectively is to compare experimental and simulated vibrational spectra. The frequencies of the vibrations reflect the bonding of the system of interest and even a qualitative analysis of intensities can be informative as the IR band intensities probe the effectiveness of the calculation in terms of modelling dipoles. The Raman intensities inform of how effectively polarisability is modelled, which is biased to the frontier molecular orbitals.^[44–46]

The FTIR and FT-Raman spectra of the small-molecule complexes were compared with simulated data. The resulting mean absolute deviations (MADs) of the frequencies are shown in Table 4; the values are indicative of satisfactory calculations.^[29,43–45,47–51]

Table 4. Mean absolute deviations (MADs) between experimental and calculated data.

	MAD	
	Raman [cm^{-1}]	IR [cm^{-1}]
$[(\text{L}^1\text{-H})\text{PtCl}]$	6	10
$[(\text{L}^1\text{-H})\text{PdCl}]$	6	9
$[(\text{L}^4\text{-H})\text{PtCl}]$	7	10
$[\text{L}^5\text{Re}(\text{CO})_3\text{Cl}]$	8	9
$[(\text{L}^5\text{-H})\text{PtCl}]$	4	10

Infrared Spectra

The infrared spectra of all the metal complexes are very dependent on the ligand. Complexes with the same ligand appear almost identical, for example, $[(\text{L}^5\text{-H})\text{PtCl}]$ and $[\text{L}^5\text{Re}(\text{CO})_3\text{Cl}]$, with any differences arising solely from the variation of the phenoxy and 2,2'-oxybiphenyl attachments on the phosphazene units of L^1 and L^4/L^5 , respectively. All the spectra are dominated by a broad peak at around

1174 cm^{-1} , which corresponds to hydrogen bending modes on the phenoxy or 2,2'-oxybiphenyl units. Furthermore, for complexes containing L^4 and L^5 , large peaks are observed at 1488 and 950 cm^{-1} , assigned to hydrogen stretching and delocalised 2,2'-oxybiphenyl vibrations, respectively. Complexes containing L^1 show peaks at 1096 and 888 cm^{-1} , which correspond to hydrogen stretching and delocalised phenoxy vibrations. The spectra of the polymers are very similar. Compared with the small-molecule spectra, the dominant peak is shifted to 1214 cm^{-1} and many peaks appear broadened. Carbonyl stretches are observed as strong peaks in the FTIR spectra of the rhenium compounds $[\text{L}^5\text{Re}(\text{CO})_3\text{Cl}]$ and $[\text{L}^6\text{Re}(\text{CO})_3\text{Cl}]$. Back-bonding from the metal d orbitals to the carbonyl anti-bonding orbitals causes a decrease in the $\text{C}\equiv\text{O}$ stretching frequency, which may give an insight into the electron density at the metal centre. Both the small-molecule complex $[\text{L}^5\text{Re}(\text{CO})_3\text{Cl}]$ and the polymer $[\text{L}^6\text{Re}(\text{CO})_3\text{Cl}]$ show identical peaks at 2023 , 1922 and 1890 cm^{-1} , which are themselves within 5 cm^{-1} of those observed for $[\text{Re}(\text{Ph}_2\text{bpy})(\text{CO})_3\text{Cl}]$.^[52] The discrepancy in frequencies is within experimental error. This suggests a minimal electronic effect of the phosphazene on the chromophore, be it the polymeric or small-molecule variants, and also gives some confidence in the use of cyclotriphosphazenes as computationally and spectroscopically manageable analogues for the study of polymeric systems.

Electronic Absorption, Emission and Lifetime Data

The electronic absorption, emission and lifetime data for selected compounds are summarised in Table 5 and Table S2. The absorption spectra of the platinum complexes are comparable to that of $[(4,6\text{-diphenyl-bpy})\text{PtCl}]$.^[53] A low-energy tail at around $500\text{--}520\text{ nm}$ is assigned as a d–d transition, moderate-energy bands at around $400\text{--}450\text{ nm}$ can be attributed to a metal-to-ligand charge-transfer (MLCT) transition and higher-energy bands at around 330 nm are due to ligand-centred transitions. This is also consistent with resonance Raman assignments (see below). In addition, high-energy peaks observed at around 245 nm for $[(\text{L}^4\text{-H})\text{PtCl}]$ and $[(\text{L}^5\text{-H})\text{PtCl}]$ can be assigned to transitions in the 2,2'-oxybiphenyl units attached to the phosphazene. This peak is absent for compounds containing L^1 in which phenoxy groups are present instead. For compound $[(\text{L}^1\text{-H})\text{PdCl}]$, the d–d and MLCT transitions are blueshifted to 424 and 398 nm , respectively, which is similar to $[(4,6\text{-diphenyl-bpy})\text{PdCl}]$.^[54] An absorption blueshift for analogous Pt and Pd complexes has previously been reported and is attributed to a higher ionisation potential of the frontier d orbitals of the latter metal.^[54,55] $[\text{L}^6\text{Re}(\text{CO})_3\text{Cl}]$ is very similar to an analogous compound that lacks the phenyl substituent at the 6-position reported earlier.^[29] This suggests that the dihedral angle between the phenyl and bpy is great enough to disrupt conjugation across this part of the ligand in the ground state. The absorption spectra of the phosphazene polymers are very sim-

ilar to those of the corresponding small-molecule complexes. The main difference lies in decreased molar absorptivities, which is explained by their lower chromophore densities. This is evidence that no electronic communication exists across the polyphosphazene chain.

Table 5. Electronic absorption, emission and lifetime data for selected compounds in dichloromethane at 298 K.

	λ_{abs} [nm] (ϵ [$10^3 \text{ L mol}^{-1} \text{ cm}^{-1}$])	λ_{em} [nm]	τ [ns]
[(L ¹ -H)PtCl]	512 sh (0.44), 437 (5.0), 419 sh (4.8), 365 (9.7), 332 (22), 292 (45)	572	270 ± 10
[(L ¹ -H)PdCl]	424 sh (0.53), 398 sh (1.5), 347sh (16), 330 (24), 291 (49)	564	–
[(L ⁴ -H)PtCl]	512 sh (0.49), 436 (4.5), 419 sh (4.2), 364 (8.9), 335 (19)	572	270 ± 10
[(L ⁵ -H)PtCl] ^[a]	506 sh (0.49), 437sh (3.3), 415 (3.4), 367 sh (7), 332 (14), 282 (32)	572	280 ± 10
[L ⁵ Re(CO) ₃ Cl]	394 (4.4), 301 (24)	634	27 ± 5
[L ⁶ Re(CO) ₃ Cl]	383 (1.2), 304 (5.8), 267 (7.6)	619	60 ± 10
[(L ⁶ -H)PtCl]	516 sh (0.03), 428 (0.2), 368 (11)	568	210 ± 40

[a] Emission of [(L¹-H)PdCl] was too weak for lifetime acquisition.

Emission and lifetime properties are important for the design of OLEDs. Comparisons with complexes that do not contain phosphazenes are thus useful to ascertain whether phosphazenes are suitable for these devices. Emission appears to be solely dependent on the metal centre, the platinum and rhenium compounds emitting most strongly at 572 and 634 nm, respectively, in dichloromethane. This is comparable to the data for similar complexes published in the literature, for which emission is observed at 564 and 629 nm, respectively.^[29,52,53] Lifetimes, however, are somewhat shorter, giving decay constants of around 270 ns for the platinum complexes and 27 ns for the rhenium complex, which compares with around 500 and 47 ns, respectively, for similar compounds in the literature.^[29,53] For [L⁶Re(CO)₃Cl], this can be attributed to the extra phenyl group at the 6-position of bpy, however, no significant structural changes exist for the platinum chromophores. For both the emission and lifetimes, the polymers have values close to their discrete small-molecule counterparts.

Resonance Raman Spectra

Resonance Raman spectroscopy may be used to identify the absorbing chromophore for a specific electronic excitation. Normal modes that mimic ground-to excited-state geometry changes are preferentially enhanced in intensity and this enables unambiguous assignments to be made of chromophorically active regions in a molecule.^[44,47,56,57] Figure 5 shows the resonance Raman spectra of [(L¹-H)-PtCl] at a number of excitation wavelengths. These are representative of the compounds [(L⁴-H)PtCl] and [(L⁵-H)-PtCl] as the spectra are almost identical. Furthermore, for all the compounds, the spectra acquired at 406.7 and 457.9 nm are very similar to those at 413.1 and 444.3 nm,

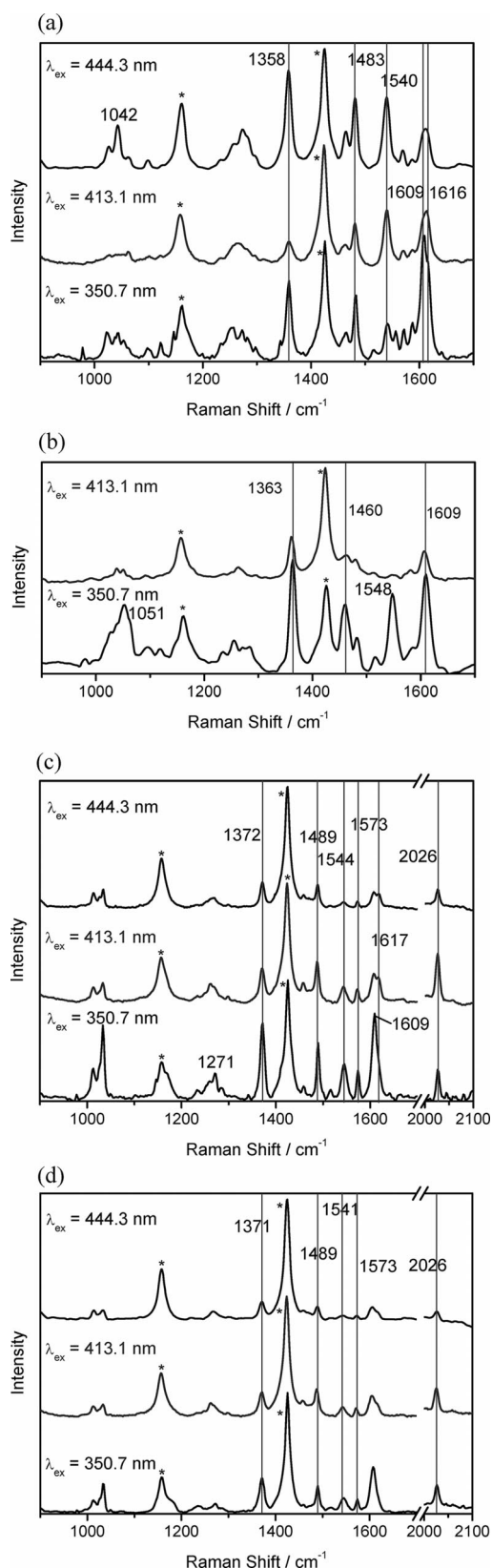


Figure 5. Resonance Raman spectra acquired in dichloromethane at a number of excitation wavelengths. (a) Spectra of [(L¹-H)PtCl], which are also representative of [(L⁴-H)PtCl] and [(L⁵-H)PtCl]. (b) Spectra of [(L¹-H)PdCl]. (c) Spectra of [L⁵Re(CO)₃Cl]. (d) Spectra of the polymeric compound [L⁶Re(CO)₃Cl]. Solvent peaks are marked by asterisks.

respectively, and have therefore been omitted for clarity. The spectrum of $[(L^1-H)PtCl]$ acquired at 350.7 nm shows resonance-enhancement at 1358, 1483 and around 1610 cm^{-1} , which are identified as modes delocalised over the entire OPhbpyPh unit with significant contributions from both Ph units. In the spectra acquired at 444.3 nm and higher wavelengths, the peaks at 1042 and 1540 cm^{-1} show strong relative enhancement. This is consistent with the probing of two different electronic states and these peaks are associated with an MLCT excited state due to their localisation on the bpy portion of the ligand (an example is shown in Figure 6, a). The spectra acquired at 406.7 and 413.1 nm are intermediate between the higher- and lower-energy spectra. The relative intensities of the solvent bands are greater because this wavelength region corresponds to a dip in the absorption spectrum between two peaks. The spectrum of $[(L^1-H)PdCl]$ shows some similar peak frequencies but different intensities compared with the platinum compounds. MLCT transition marker bands at 1051

and 1548 cm^{-1} (comparable to the bands at 1042 and 1540 cm^{-1} , respectively, for the platinum spectra) are observed at an excitation wavelength of 350.7 nm, however, they diminish rapidly at higher wavelengths. This is consistent with a blueshift of the MLCT band until it overlaps with the $\pi \rightarrow \pi^*$ transition caused by lower metal d-orbital energies.

The spectra of the rhenium compound $[L^5Re(CO)_3Cl]$ are different to those of the platinum and palladium compounds due to two-coordinate binding of Re to L^5 compared with three-coordinate binding of L^5 , L^4 or L^1 to the other metals. The resonance Raman spectra generated with 350.7 nm excitation shows a number of bands similar to $[Re(bpy)(CO)_3Cl]$, but in addition new or significantly shifted features are observed at 1358, 1544 and 1609 cm^{-1} . Analysis of these shows the involvement of 6-Ph or 4-PhO moieties in the normal modes, as shown in parts b and c of Figure 6. Also notable is the emergence of a peak at 1617 cm^{-1} at excitation wavelengths of 406.7 nm and longer, which corresponds to somewhat more localised bpy vibrations. This, and the presence of a $C \equiv O$ stretching-peak at 2026 cm^{-1} , which shows higher relative intensities in the lower-energy spectra, supports the assignment of the absorption band at 394 nm as a MLCT transition.

The polymer spectra are very similar to their small-molecule counterparts, showing peaks at the same wavenumbers and with the same relative intensities, which suggests the same state is probed in each case. Note that solvent peaks appear more marked due to lower chromophore densities compared with the monomers.

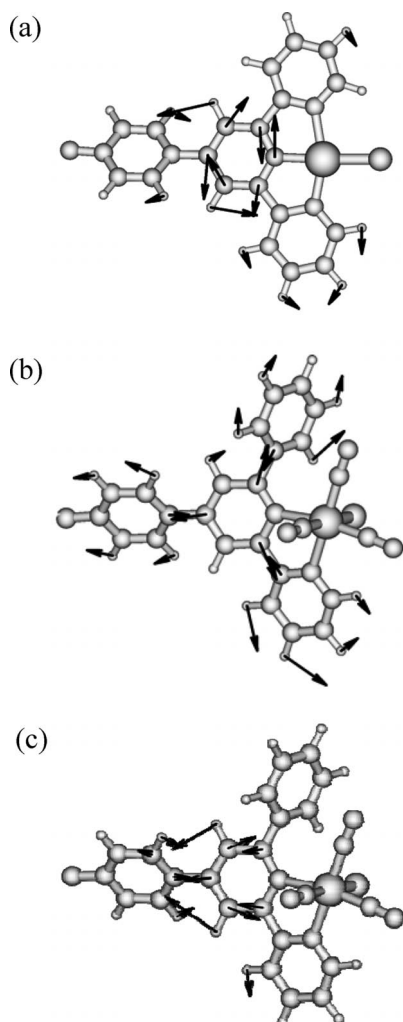


Figure 6. Normal-mode diagrams depicting the vibrations of (a) $[(L^1-H)PtCl]$ at 1540 cm^{-1} , (b) $[L^5Re(CO)_3Cl]$ at 1358 cm^{-1} and (c) $[L^5Re(CO)_3Cl]$ at 1609 cm^{-1} . The cyclotriphosphazene unit has been omitted for clarity as no activity is observed in any other part of the complex for this mode.

Transient Resonance Raman Spectroscopy

The use of transient resonance Raman spectroscopy enables the direct observation of the excited state of a compound. The sample is excited by using the leading edge of a laser pulse and near-simultaneously probed by using the trailing edge of the pulse. A number of excited-state species have characteristic peaks, for example, bpy peaks can be observed in the excited states of $[Ru(bpy)_3]^{2+}$ as well as $[Re(bpy)(CO)_3Cl]$.^[58] The spectra collected for compounds $[(L^1-H)PtCl]$, $[(L^5-H)PtCl]$ and $[(L^4-H)PtCl]$ are very similar and are represented by the spectrum of the latter in Figure 7, which shows several excited-state features. Three different pulse energies were used to monitor their growth and a plot of the log of the peak intensity against the log of power results in a line with a gradient of one. In a situation in which there is partial excited-state population, non-linear behaviour is observed.^[59] However, in this case, in which the excited-state lifetime is long compared with the laser pulse duration, saturation of the excited-state population within the irradiated sample volume is observed. This is consistent with the photon-to-molecule ratio, which is around 30 for the highest pulse energy.^[60] Excited-state features are observed at 1042, 1465, 1547 and, after solvent-subtraction, at 1171 cm^{-1} . Some of these peaks appear at frequencies similar to the stretching vibrations of the bpy^-

radical anion observed in the excited-states of $[\text{Ru}(\text{bpy})_3]^{2+}$ and $[\text{Re}(\text{bpy})(\text{CO})_3\text{Cl}]$.^[58] However, assignment of these peaks to $\text{bpy}^{\cdot-}$ is precluded by the absence of several characteristic bands, most notably a strong feature normally observed at 1283 cm^{-1} . As a result of the tridentate nature of the ligand this is not surprising and we assign the excited-state features to a $\text{OPhbpPh}^{\cdot-}$ state.

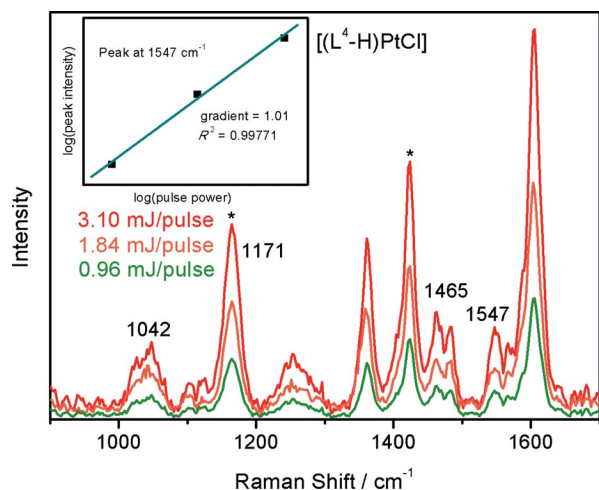


Figure 7. Transient resonance Raman spectra of $[(\text{L}^4\text{-H})\text{PtCl}]$ at a number of pulse energies. The inset shows the growth of the peak at 1547 cm^{-1} with respect to pulse power.

Conclusions

Ground- and excited-state studies have been carried out on discrete and polymeric phosphazene compounds. UV/Vis and resonance Raman analyses show high-energy $\pi \rightarrow \pi^*$ transitions at around 330 nm located in the bipyridyl-based portion of the ligand and lower-energy MLCT transitions for the platinum and rhenium complexes. There is little deviation from analogous compounds lacking the phosphazene substituents. Transient resonance Raman spectra of the platinum complexes show excited-state features that are distinct from the radical anion of bipyridine. Furthermore, we have shown that the cyclotriphosphazene complexes are appropriate for modelling the behaviour of the polyphosphazenes as there is little deviation in the photophysics between the two classes of compounds. The findings suggest that material and photophysical properties of polyphosphazenes can be effectively decoupled from one another; that is, independent control is possible. By extension, it should be possible to incorporate other properties such as catalysis while retaining control over parameters such as T_g , solubility and chemical stability.

Experimental Section

General: Analytical-grade solvents were used as received with the exception of tetrahydrofuran (THF), which was distilled from sodium/benzophenone. Tetrabutylammonium bromide (TBAB) was

obtained from Merck and $[\text{Re}(\text{CO})_5\text{Cl}]$ was obtained from the Pressure Chemical Co. (Pittsburgh). (Pentaphenoxy)[4-(6-phenyl-2,2'-bipyridin-4-yl)phenoxy]cyclotriphosphazene (L^1),^[29] 4-(4-hydroxyphenyl)-6-phenyl-2,2'-bipyridine (HOPhbpPh),^[61] $[(\text{L-H})\text{PtCl}]$ ($\text{L} = \text{HOPhbpPh}$),^[7] $[\text{Pt}(\text{PhCN})_2\text{Cl}_2]$,^[62] $[\text{Pd}(\text{PhCN})_2\text{Cl}_2]$,^[63] $\text{N}_3\text{P}_3(\text{OPh})_5\text{Cl}$ ($\text{OPh} = \text{phenoxy}$),^[64] $\text{N}_3\text{P}_3(\text{biph})_2\text{Cl}_2$ ($\text{biph} = 2,2'$ -oxybiphenyl),^[65] $\text{N}_3\text{P}_3(\text{tBubiph})_2\text{Cl}_2$ ($\text{tBubiph} = 4,4'$ -di-*tert*-butyl-2,2'-oxybiphenyl),^[31] and $(\text{NPCl}_2)_n$ ^[22] were prepared according to literature procedures.

^1H NMR spectra were recorded at 162 MHz and $^{31}\text{P}\{^1\text{H}\}$ NMR spectra at 400 MHz with a Bruker Advance 400 spectrometer. Electrospray mass spectra were obtained from CH_3CN solutions with a Micromass ZMD spectrometer run in the positive ion mode. Listed peaks correspond to the most abundant isotopomer; assignments were made by a comparison of observed and simulated spectra. IR spectra were recorded as KBr discs with a Perkin–Elmer FT-IR Paragon 1000 spectrometer and electronic absorption spectra were recorded with a Shimadzu UV-160A spectrometer. Glass transition temperatures were measured with a TA Instruments Q10 differential scanning calorimetry apparatus at a heating rate of $10\text{ }^\circ\text{C}/\text{min}$ and with a sample size of around 10 mg . Gel permeation chromatograms were obtained by using a Hewlett–Packard HP 1100 gel permeation chromatograph equipped with two Phenomenex Phenogel linear $10\text{ }\mu\text{m}$ columns and a Hewlett–Packard 1047A refractive index detector. The samples were eluted at $1.0\text{ mL}/\text{min}$ with a 10 mM solution of tetra-*n*-butylammonium nitrate in THF and the elution times were calibrated with polystyrene standards. Microanalyses were performed by the Campbell Microanalytical Laboratory, University of Otago.

FT-Raman spectra were acquired by using a Bruker Equinox 55 interferometer coupled with a FRA-106 Raman module and a DT418T liquid-nitrogen cooled Germanium detector. A 1064 nm Nd:YAG laser operating at 450 mW was used as the source. The samples were pressed into KBr disks. Resonance Raman spectra were recorded in 10^{-3} mol/L CH_2Cl_2 solutions using a set-up previously described.^[48,66] In short, the excitation beam and collection lens are in a 135° backscattering arrangement. Scattered photons were focused on the entrance slit of an Acton SpectraPro500i spectrograph with a $1200\text{ grooves}/\text{mm}$ grating, which disperses the radiation in a horizontal plane on a Princeton Instruments Spec10 liquid-nitrogen-cooled CCD detector. A Coherent Innova I-302 krypton ion laser was used to provide excitation wavelengths (λ_{ex}) of 350.7 , 406.7 and 413.1 nm , a solid-state CrystaLaser for 444.3 nm and a Melles Griot OmNihrome argon-ion laser for 457.9 , 488.0 and 514.5 nm . Notch filters matched to these wavelengths were used to remove the laser excitation line. Transient resonance Raman signals were acquired by using a single pulse of a Brilliant (Quantel) Nd:YAG pulse laser operating at $\lambda_{\text{ex}} = 354.7\text{ nm}$ to excite and probe the sample. A similar set-up but with a $300\text{ grooves}/\text{mm}$ grating was used to perform continuous-emission spectroscopy at $\lambda_{\text{ex}} = 350.7\text{ nm}$. Lifetime measurements were obtained by excitation using the Brilliant laser described above. The emission transients were recorded by a Hamamatsu H5783-04 photomultiplier at 580 , 620 , 660 and 700 nm and read out on a TDS 3032B (Tektronix) digital oscilloscope. The errors were estimated by using the standard deviation between each wavelength. Typically, the natural logarithm of the data could be fit linearly with R^2 values greater than 0.95 .

Ligand Synthesis

$\text{N}_3\text{P}_3(\text{biph})_2(\text{OPhbpPh})_2$ (L^2): A mixture of HOPhbpPh (325 mg , 1.0 mmol) and NaH (40 mg of a 60% dispersion in oil) in THF (30 mL) was stirred at room temperature over 1 h . $\text{P}_3\text{N}_3(\text{biph})_2\text{Cl}_2$

(288 mg, 0.5 mmol) and TBAB (30 mg) were added and the mixture was heated at reflux overnight. The THF was removed in a rotary evaporator, the residue extracted with CH_2Cl_2 and the extract filtered through Celite. Chromatography on silica using MeOH (0–2%) in CH_2Cl_2 as eluent yielded the product as a white powder, which was recrystallised from CH_2Cl_2 /hexane and dried under vacuum; yield 361 mg (63%). ^1H NMR (CDCl_3): δ = 8.74–8.64 (m, 6 H), 8.19–8.16 (m, 4 H), 7.99 (s, 2 H), 7.56–7.36 (m, 20 H), 7.13–7.11 (m, 4 H) ppm. $^{31}\text{P}\{^1\text{H}\}$ NMR (CDCl_3): δ = 25.43 (d, J_{PP} = 93 Hz, 2 P), 9.66 (t, J_{PP} = 91 Hz, 1 P) ppm. IR: $\tilde{\nu}_{\text{max}}$ = 1230 (s), 1173 (vs) cm^{-1} . MS (ES): m/z = 1150 [$\text{L}^2 + \text{H}$] $^+$. $\text{C}_{68}\text{H}_{46}\text{N}_7\text{O}_6\text{P}_3$ (1150.06): calcd. C 71.02, H 4.03, N 8.53; found C 70.79, H 4.22, N 8.56.

$\text{N}_3\text{P}_3(\text{tBubiph})_2(\text{OPhbpPh})_2$ (L^3): A mixture of HOPhbpPh (162 mg, 0.5 mmol) and NaH (20 mg of a 60% dispersion in oil, 0.5 mmol NaH) in THF (30 mL) was stirred at room temperature over 1 h. $\text{P}_3\text{N}_3(\text{tBubiph})_2\text{Cl}_2$ (198 mg, 0.25 mmol) and TBAB (30 mg) were added and the mixture was heated at reflux overnight. The THF was removed in a rotary evaporator, the residue extracted with CH_2Cl_2 and the extract filtered through Celite. Chromatography on silica using MeOH (0–2%) in CH_2Cl_2 as eluent yielded the product as a white powder, which was recrystallised from CH_2Cl_2 /hexane and dried under vacuum; yield 270 mg (79%). ^1H NMR (CDCl_3): δ = 8.72–8.64 (m, 6 H), 8.19 (m, 4 H), 8.00 (m, 2 H), 7.90–7.82 (m, 6 H), 7.56 (m, 4 H), 7.51 (m, 4 H), 7.44 (m, 6 H), 7.38 (m, 4 H), 7.32 (m, 2 H), 7.03 (m, 4 H), 1.32 (s, 36 H) ppm. $^{31}\text{P}\{^1\text{H}\}$ NMR (CDCl_3): δ = 25.4 (d, J_{PP} = 92 Hz, 2 P), 10.0 (t, J_{PP} = 92 Hz, 1 P) ppm. IR: $\tilde{\nu}_{\text{max}}$ = 1230 (s), 1201 (vs), 1184 (vs) cm^{-1} . MS (ES): m/z = 1375 [$\text{L}^3 + \text{H}$] $^+$. $\text{C}_{84}\text{H}_{78}\text{N}_7\text{O}_6\text{P}_3$ (1374.48): calcd. C 73.40, H 5.72, N 7.13; found C 73.12, H 5.91, N 7.13.

$\text{N}_3\text{P}_3(\text{biph})_2(\text{OPhbpPh})\text{Cl}$ (L^4): A mixture of HOPhbpPh (243 mg, 0.75 mmol) and NaH (20 mg of a 60% dispersion in oil, 0.5 mmol NaH) in THF (35 mL) was stirred at room temperature over 1 h. $\text{P}_3\text{N}_3(\text{biph})_2\text{Cl}_2$ (473 mg, 0.83 mmol) and TBAB (20 mg) were added and the mixture was heated at reflux over 5 h. The THF was removed in a rotary evaporator, the residue extracted with CH_2Cl_2 and the extract filtered through Celite. Chromatography on silica using MeOH (0–2%) in CH_2Cl_2 as eluent yielded the product as a white solid, which was dried under vacuum at 75 °C; yield 580 mg (89%). ^1H NMR (CDCl_3): δ = 8.70–8.64 (m, 2 H), 8.61 (m, 1 H), 8.18 (m, 2 H), 7.93 (m, 1 H), 7.88–7.80 (m, 3 H), 7.55–7.48 (m, 8 H), 7.48–7.23 (m, 12 H), 7.24 (m, 2 H) ppm. $^{31}\text{P}\{^1\text{H}\}$ NMR (CDCl_3): δ = 22.70 (s, 3 P) ppm. IR: $\tilde{\nu}_{\text{max}}$ = 1232 (s), 1176 (vs) cm^{-1} . MS (ES): m/z = 862 [$\text{L}^4 + \text{H}$] $^+$. $\text{C}_{46}\text{H}_{31}\text{ClN}_5\text{O}_5\text{P}_3$ (862.14): calcd. C 64.08, H 3.62, N 8.12; found C 64.18, H 3.87, N 7.95.

$\text{N}_3\text{P}_3(\text{biph})_2(\text{OPhbpPh})(\text{OPh})$ (L^5): To a solution of phenol (33 mg, 0.35 mmol) in THF (20 mL), NaH (15 mg of a 60% dispersion in oil, 0.35 mmol NaH) was added and the mixture was stirred over 0.5 h. L^4 (300 mg, 0.35 mmol) and TBAB (10 mg) were added and the mixture was heated at reflux overnight. The THF was removed in a rotary evaporator, the residue extracted with CH_2Cl_2 and the extract filtered through Celite. Chromatography on silica using CH_2Cl_2 /MeOH (0–2%) as eluent gave a white powder that was recrystallised from CH_2Cl_2 /hexane and dried under vacuum at 75 °C; yield 248 mg (78%). ^1H NMR (CDCl_3): δ = 8.71–8.62 (m, 3 H), 8.18 (m, 2 H), 7.98–7.95 (m, 1 H), 7.89–7.82 (m, 3 H), 7.58–7.23 (m, 24 H), 7.13–7.01 (m, 2 H), 7.03 (m, 2 H) ppm. $^{31}\text{P}\{^1\text{H}\}$ NMR (CDCl_3): δ = 25.5 (m, 2 P), 9.7 (m, 1 P) ppm. IR: $\tilde{\nu}_{\text{max}}$ = 1230 (s), 1175 (vs) cm^{-1} . MS (ES): m/z = 920 [$\text{L}^5 + \text{H}$] $^+$. $\text{C}_{52}\text{H}_{36}\text{N}_5\text{O}_6\text{P}_3$ (919.79): calcd. C 67.90, H 3.94, N 7.61; found C 68.51, H 4.18, N 7.76.

Complex Synthesis

$[(\text{L}^1\text{-H})\text{PdCl}]$: A solution of L^1 (92 mg, 0.1 mmol) and $[\text{Pd}(\text{PhCN})_2\text{Cl}_2]$ (38 mg, 0.1 mmol) in MeOH/benzene (1:1, 15 mL) was heated at reflux overnight. The solution was taken to dryness in a rotary evaporator to give a yellow oil, which formed a yellow powder when triturated with MeOH. The powder was recrystallised from CH_2Cl_2 /hexane and dried under vacuum at 75 °C; yield 50 mg. ^1H NMR (CDCl_3): δ = 8.61 (m, 1 H), 7.99 (m, 1 H), 7.90 (m, 1 H), 7.66 (s, 1 H), 7.62 (m, 1 H), 7.55 (m, 2 H), 7.40 (s, 1 H), 7.35 (m, 1 H), 7.28–7.11 (m, 18 H), 7.01–7.03 (m, 4 H), 7.03–6.88 (m, 8 H) ppm. $^{31}\text{P}\{^1\text{H}\}$ NMR (CDCl_3): δ = 9.6–9.0 (m, 3 P) ppm. IR: $\tilde{\nu}_{\text{max}}$ = 1242 (s), 1203 (vs), 1175 (vs), 1160 (vs) cm^{-1} . $\text{C}_{52}\text{H}_{39}\text{ClN}_5\text{O}_6\text{P}_3\text{Pd}$ (1064.69): calcd. C 58.66, H 3.69, N 6.58; found C 58.55, H 3.70, N 6.51.

$[(\text{L}^1\text{-H})\text{PtCl}]$: A solution of L^1 (125 mg, 1.4 mmol) and $[\text{Pt}(\text{PhCN})_2\text{Cl}_2]$ (64 mg, 1.4 mmol) in MeOH/benzene (1:1, 15 mL) was heated at reflux overnight. The solution was taken to dryness in a rotary evaporator to give a yellow oil. Vapour diffusion of pentane into a solution of the oil in CHCl_3 gave the complex as an orange precipitate, which was dried under vacuum at 75 °C; yield 100 mg. ^1H NMR (CDCl_3): δ = 8.79 (m, 1 H), 7.97–7.85 (m, 2 H), 7.64–7.47 (m, 4 H), 7.40 (m, 1 H), 7.31–7.10 (m, 19 H), 7.09–7.04 (m, 4 H), 7.03–6.95 (m, 4 H), 6.94–6.90 (m, 4 H) ppm. $^{31}\text{P}\{^1\text{H}\}$ NMR (CDCl_3): δ = 8.9–8.4 (m, 3 P) ppm. IR: $\tilde{\nu}_{\text{max}}$ = 1234 (s), 1202 (vs), 1193 (vs), 1174 (vs), 1160 (vs) cm^{-1} . $\text{C}_{52}\text{H}_{39}\text{ClN}_5\text{O}_6\text{P}_3\text{Pt}$ (1153.35): calcd. C 54.15, H 3.41, N 6.07; found C 53.85, H 3.50, N 5.98.

$[(\text{L}^2\text{-H})(\text{PdCl})_2]$: A mixture of L^2 (75 mg, 0.65 mmol) and $[\text{Pd}(\text{PhCN})_2\text{Cl}_2]$ (50 mg, 1.31 mmol) in MeOH/benzene (1:1, 15 mL) was heated at reflux overnight. A yellow precipitate formed that was collected by filtration, washed with CH_2Cl_2 and Et_2O , recrystallised from DMSO and dried under vacuum at 75 °C; yield 60 mg. ^1H NMR ($[\text{D}_6]\text{DMSO}$): δ = 8.66 (m, 2 H), 8.57–8.51 (m, 4 H), 8.32–8.25 (m, 6 H), 8.24–8.17 (m, 2 H), 7.76 (m, 2 H), 7.71 (m, 2 H), 7.65 (m, 4 H), 7.57 (m, 4 H), 7.51 (m, 4 H), 7.43 (m, 6 H), 7.22 (m, 4 H), 7.01 (m, 4 H) ppm. $^{31}\text{P}\{^1\text{H}\}$ NMR ($[\text{D}_6]\text{DMSO}$): δ = 25.3 (d, J_{PP} = 92 Hz, 2 P), 9.8 (t, J_{PP} = 92 Hz, 1 P) ppm. IR: $\tilde{\nu}_{\text{max}}$ = 1230 (s), 1169 (vs) cm^{-1} . $\text{C}_{68}\text{H}_{44}\text{Cl}_2\text{N}_7\text{O}_6\text{P}_3\text{Pd}_2$ (1431.79): calcd. C 57.04, H 3.10, N 6.85; found C 56.77, H 3.30, N 6.63.

$[(\text{L}^3\text{-H})(\text{PdCl})_2]\cdot 0.5\text{DMSO}$: A mixture of L^3 (69 mg, 0.05 mmol) and $[\text{Pd}(\text{PhCN})_2\text{Cl}_2]$ (38 mg, 0.1 mmol) in MeOH/benzene (1:1, 15 mL) was heated at reflux overnight. A yellow precipitate formed that was collected by filtration and washed with Et_2O . Purification was achieved by vapour diffusion of MeOH into a DMSO solution of the precipitate, which was dried under vacuum. ^1H NMR ($[\text{D}_6]\text{DMSO}$): δ = 8.75 (m, 2 H), 8.68–8.62 (m, 4 H), 8.42–8.26 (m, 8 H), 7.86 (m, 2 H), 7.81 (m, 2 H), 7.65–7.60 (m, 8 H), 7.57–7.52 (m, 6 H), 7.18–7.07 (m, 8 H), 1.34 (s, 36 H) ppm. $^{31}\text{P}\{^1\text{H}\}$ NMR ($[\text{D}_6]\text{DMSO}$): δ = 25.07 (d, J_{PP} = 93 Hz, 2 P), 9.97 (t, J_{PP} = 93 Hz, 1 P) ppm. IR: $\tilde{\nu}_{\text{max}}$ = 1230 (s), 1181 (vs) cm^{-1} . $\text{C}_{85}\text{H}_{79}\text{Cl}_2\text{N}_7\text{O}_7.5\text{P}_3\text{Pd}_2\text{S}_{0.5}$ (1734.34): calcd. C 60.17, H 4.66, N 5.78; found C 60.08, H 4.66, N 5.88.

$[(\text{L}^4\text{-H})\text{PtCl}]$: A mixture of $[(\text{L-H})\text{PtCl}]$ ($\text{L} = \text{HOPhbpPh}$) (55 mg, 0.1 mmol), $\text{N}_3\text{P}_3(\text{biph})_2\text{Cl}_2$ (57 mg, 0.1 mmol) and Cs_2CO_3 (300 mg, 0.9 mmol) in acetone was stirred at reflux overnight. The reaction mixture was taken to dryness in a rotary evaporator, the residue extracted with CH_2Cl_2 and then filtered through Celite. Addition of hexane to the filtrate caused an orange complex to precipitate that was collected by filtration and dried under vacuum; yield 55 mg. ^1H NMR (CDCl_3): δ = 8.80 (m, 1 H), 7.90 (m, 2 H), 7.72 (m, 2 H), 7.62–7.47 (m, 12 H), 7.45–7.32 (m, 10 H), 7.20 (m, 1 H), 7.02 (m, 1 H), 7.00 (m, 1 H) ppm. IR: $\tilde{\nu}_{\text{max}}$ = 1231 (s), 1174

(vs) cm^{-1} . $\text{C}_{46}\text{H}_{30}\text{Cl}_2\text{N}_5\text{O}_5\text{P}_3\text{Pt}$ (1091.67): calcd. C 50.61, H 2.77, N 6.42; found C 50.26, H 2.84, N 6.31.

[(L⁵-H)PtCl]: A mixture of L⁵ (92 mg, 0.1 mmol) and [Pt(PhCN)₂Cl₂] (47 mg, 0.1 mmol) in MeOH/benzene (1:1, 15 mL) was heated at reflux overnight. An orange precipitate formed that was collected by filtration, washed with Et₂O and dried under vacuum at 75 °C; yield 47 mg. The filtrate was taken to dryness, redissolved in MeOH/benzene (1:1, 15 mL) and heated for a further 2 d at reflux to yield a second crop of the complex (30 mg). ¹H NMR (CDCl₃): δ = 8.74 (m, 1 H), 7.88–7.80 (m, 2 H), 7.71 (m, 2 H), 7.58–7.36 (m, 17 H), 7.36–7.26 (m, 7 H), 7.23 (m, 2 H), 7.15 (m, 1 H), 7.07 (m, 2 H), 7.03–7.68 (m, 2 H) ppm. ³¹P{¹H} NMR (CDCl₃): δ = 25.60 (d, J_{PP} = 92 Hz, 2 P), 9.76 (m, 1 P) ppm. IR: $\tilde{\nu}_{\text{max}}$ = 1230 (s), 1176 (vs). $\text{C}_{52}\text{H}_{35}\text{ClN}_5\text{O}_6\text{P}_3\text{Pt}$ (1149.32): calcd. C 54.34, H 3.07, N 6.09; found C 54.46, H 3.17, N 6.14.

[L⁵Re(CO)₃Cl]: A mixture of L⁵ (50 mg, 0.54 mmol) and [Re(CO)₅Cl] (20 mg, 0.55 mmol) in toluene was heated at reflux over 5 h. The solution was filtered while hot and after standing for 3 d a yellow precipitate developed that was collected by filtration, washed with Et₂O and dried under vacuum; yield 60 mg. ¹H NMR (CDCl₃): δ = 9.09 (m, 1 H), 8.68–8.61 (m, 2 H), 8.22 (m, 1 H), 8.13 (m, 2 H), 7.98 (m, 1 H), 7.74–7.68 (m, 2 H), 7.66–7.54 (m, 11 H), 7.53–7.36 (m, 10 H), 7.29 (m, 1 H), 7.24–7.15 (m, 3 H), 7.11 (m, 2 H) ppm. ³¹P{¹H} NMR (CDCl₃): δ = 25.38 (d, J_{PP} = 97 Hz, 2 P), 10.54 (m, 1 P) ppm. IR: $\tilde{\nu}_{\text{max}}$ = 2023 (vs), 1922 (vs), 1890 (vs), 1231 (s), 1200 (s), 1171 (vs) cm^{-1} . $\text{C}_{55}\text{H}_{36}\text{ClN}_5\text{O}_6\text{P}_3\text{Re}$ (1225.48): calcd. C 53.90, H 2.96, N 5.71; found C 54.78, H 3.08, N 5.57.

Polymer Synthesis

{[NP(OrBuPh)₂]_{0.75-x}[NP(OrBuPh)(OPhbpPh)]_{0.25}[NP(OrBuPh)Cl]_x]_n (L⁶): Cs₂CO₃ (7 g, 20 mmol) and HOPhbpPh (420 mg, 1.2 mmol) were added to a solution containing (NPCl₂)_n (580 mg, 5 mmol) in THF (150 mL) and the mixture was heated at reflux over 24 h. *t*BuPhOH (1.7 g, 11.3 mmol) was added and the mixture was heated at reflux for a further 24 h and then TBAB (0.1 g) was added and the heating continued for 7 d. The mixture was concentrated in a rotary evaporator and the crude polymer precipitated on addition of the concentrated mixture to water (1 L). Further precipitation of concentrated THF solutions of the polymer in

water ($\times 2$) and EtOH ($\times 3$) were performed with the THF solution being filtered before the final EtOH precipitation. The recovered polymer was dried under vacuum; yield 700 mg. M_w = 598000. PDI = 1.97. T_g = 83 °C. ³¹P{¹H} NMR (CDCl₃): δ = -18.5 (s), -19 (br. sh) ppm. $\text{C}_{22.40}\text{H}_{25.72}\text{Cl}_{0.06}\text{N}_{1.50}\text{O}_{1.94}\text{P}$ (380.12): calcd. C 70.78, H 6.82, N 5.53, Cl 0.56 (for x = 0.06); found C 68.94, H 6.93, N 5.53, Cl 0.55.

[L⁶PtCl]: [Pt(PhCN)₂Cl₂] (31 mg, 0.66 mmol) was added to a solution containing L⁶ (100 mg, 0.26 mmol) in THF/toluene (1:1, 40 mL) and the solution was heated at reflux over 5 h, stirred at room temperature overnight and then heated at reflux for a further 5 h. The solution was filtered and concentrated to dryness in a rotary evaporator. The residue was washed thoroughly with ethanol and dried under vacuum at 40 °C; yield 90 mg. M_w = 346000. PDI = 2.42. T_g = 87 °C. ³¹P{¹H} NMR (CDCl₃): δ = -17.8 (s) ppm. $\text{C}_{22.40}\text{H}_{25.47}\text{Cl}_{0.31}\text{N}_{1.50}\text{O}_{1.94}\text{Pt}_{0.25}$ (437.50): calcd. C 61.46, H 5.88, N 4.80, Cl 2.52; found C 61.95, H 6.07, N 4.75, Cl 2.98.

[L⁶Re(CO)₃Cl]: [Re(CO)₅Cl] was added to a solution containing L⁶ (100 mg, 0.26 mmol) in THF (30 mL) and the solution was heated at reflux over 5 h. The solution was filtered and concentrated to dryness in a rotary evaporator. The residue was washed thoroughly with ethanol and dried under vacuum; yield 80 mg. M_w = 691000. PDI = 2.75. T_g = 120 °C. ³¹P{¹H} NMR (CDCl₃): δ = -18.6 (s) ppm. IR: $\tilde{\nu}_{\text{max}}$ = 2023 (vs), 1922 (vs), 1890 (vs), 1509 (vs), 1214 (br. vs), 1171 (vs) cm^{-1} . $\text{C}_{23.15}\text{H}_{25.72}\text{Cl}_{0.31}\text{N}_{1.5}\text{O}_{2.75}\text{PRe}_{0.25}$ (456.54): calcd. C 60.84, H 5.63, N 4.59, Cl 2.41; found C 61.34, H 5.98, N 4.63, Cl 1.99.

Crystallography: The X-ray data were collected with a Siemens P4 four circle diffractometer using a Siemens SMART 1 K CCD area detector. The crystals were mounted in an inert oil, transferred into the cold gas stream of the detector and irradiated with graphite-monochromated Mo- K_α (λ = 0.71073 Å) X-rays. The data were collected by using the SMART program and processed with SAINT^[67] to apply Lorentzian and polarisation corrections to the diffraction spots (three-dimensionally integrated). The crystal data are given in Table 6. The structures were solved by direct methods and refined by using the SHELXTL program.^[68] For the solution of L²·4H₂O, the electron density (316 e⁻ per cell) of the occupationally

Table 6. Selected crystallographic data for the compounds.

	L ² ·4H ₂ O	[(L ¹ -H)PdCl]	[(L ³ -H)(PdCl) ₂]·3EtOH·6DMF
Empirical formula	C ₆₈ H ₅₄ N ₇ O ₁₀ P ₃	C ₅₂ H ₃₉ ClN ₅ O ₆ P ₃ Pd	C ₁₀₈ H ₁₃₆ Cl ₂ N ₁₃ O ₁₅ P ₃ Pd ₂
M [g/mol]	1222.09	1064.64	2232.91
Crystal system	monoclinic	triclinic	monoclinic
Space group	$C2/c$	$P\bar{1}$	$P2_1/c$
a [Å]	38.2128(7)	9.5812(1)	14.5806(3)
b [Å]	11.4682(1)	11.8367(2)	23.7124(2)
c [Å]	30.5730(5)	22.0207(3)	28.5845(6)
α [°]	90	81.585(1)	90
β [°]	108.071(1)	80.197(1)	98.004(1)
γ [°]	90	68.383(1)	90
Z	8	2	4
T [K]	84(2)	84(2)	84(2)
Volume [Å ³]	12737.2(3)	2278.27(5)	9786.6(3)
ρ_{calcd} [g/cm ³]	1.275	1.552	1.515
$\mu(\text{Mo-}K_\alpha)$ [mm ⁻¹]	1.58	6.31	5.47
$2\theta_{\text{max}}$ [°]	51.5	50.7	51.36
$R(\text{int})$	0.0792	0	0.0833
Data / restraints / parameters	12065 / 333 / 867	8274 / 48 / 613	18455 / 312 / 1064
$R1$ [$I > 2\sigma(I)$]	0.0722	0.0506	0.062
$wR2$ (all data)	0.1969	0.0970	0.1664
GOF on F^2	0.960	1.102	0.911

and positionally disordered water molecules was removed by using PLATON/SQUEEZE^[69] and 2481.6.0 Å³ was left accessible by the void. Similar treatment was used for the solvent molecules in [(L³-H)(PdCl)₂]₃EtOH·6DMF for which 1278 e⁻ per cell were removed and 3160.7 Å³ was left accessible by the void.

CCDC-816708 (for L²-4H₂O), -816709 (for [(L¹-H)PdCl]) and -816710 (for [(L³-H)(PdCl)₂]₃EtOH·6DMF) contain the supplementary crystallographic data for this paper. These data can be obtained free of charge from The Cambridge Crystallographic Data Centre via www.ccdc.cam.ac.uk/data_request/cif.

Supporting Information (see also the footnote on the first page of this article): Calculated bond lengths and angles for [(L¹-H)PdCl] and TD-DFT data for selected complexes.

Acknowledgments

We thank the Massey University Research Fund for a postdoctoral fellowship (to C. A. O.) and the University of Otago for a postgraduate scholarship (to R. H.).

- [1] A. S. Abd-El-Aziz, I. Manners, *Frontiers in Transition Metal-Containing Polymers*, Wiley, Hoboken, NJ, **2007**.
- [2] I. Manners, *Synthetic Metal-Containing Polymers*, Wiley-VCH, Weinheim, **2004**.
- [3] W. K. Chan, *Coord. Chem. Rev.* **2007**, *251*, 2104–2118.
- [4] C. A. Bignozzi, V. Ferri, M. Scoconi, *Macromol. Chem. Phys.* **2003**, *204*, 1851–1862.
- [5] L. Huynh, Z. Wang, J. Yang, V. Stoeva, A. Lough, I. Manners, M. A. Winnik, *Chem. Mater.* **2005**, *17*, 4765–4773.
- [6] Z. Pang, X. Gu, A. Yekta, Z. Masoumi, J. B. Coll, M. A. Winnik, I. Manners, *Adv. Mater.* **1996**, *8*, 768–771.
- [7] C.-M. Che, J.-L. Zhang, L.-R. Lin, *Chem. Commun.* **2002**, 2556–2557.
- [8] K. Saatchi, U. O. Haefeli, *Dalton Trans.* **2007**, 4439–4445.
- [9] C. Wang, Y. Gong, N. Fan, S. Liu, S. Luo, J. Yu, J. Huang, *Colloids Surf. B* **2009**, *70*, 84–90.
- [10] A. S. Abd-El-Aziz, C. E. Carraher Jr., C. U. Pittman Jr., M. Zeldin, in: *Macromol. Containing Met. Met.-Like Elem.*, vol. 3, *Biomedical Applications* (Ed.: J. E. Sheats), Wiley, Hoboken, NJ, **2004**.
- [11] N. Madhavan, C. W. Jones, M. Weck, *Acc. Chem. Res.* **2008**, *41*, 1153–1165.
- [12] N. E. Leadbeater, M. Marco, *Chem. Rev.* **2002**, *102*, 3217–3273.
- [13] J. N. Demas, B. A. DeGraff, *Anal. Chem.* **1991**, *63*, 829A–837A.
- [14] E. Holder, B. M. W. Langeveld, U. S. Schubert, *Adv. Mater.* **2005**, *17*, 1109–1121.
- [15] C. S. K. Mak, W. K. Chan, in: *Highly Efficient OLEDs with Phosphorescent Materials* (Ed.: H. Yersin), Wiley-VCH, Weinheim, Germany, **2007**, pp. 392–362.
- [16] C. Ulbricht, B. Beyer, C. Friebe, A. Winter, U. S. Schubert, *Adv. Mater.* **2009**, *21*, 4418–4441.
- [17] R. Shunmugam, G. N. Tew, *Macromol. Rapid Commun.* **2008**, *29*, 1355–1362.
- [18] J. Jiang, W. Yang, Y. Cao, *J. Inorg. Organomet. Polym. Mater.* **2007**, *17*, 37–55.
- [19] A. C. Grimsdale, K. Leok Chan, R. E. Martin, P. G. Jokisz, A. B. Holmes, *Chem. Rev.* **2009**, *109*, 897–1091.
- [20] K. D. Ley, K. S. Schanze, *Coord. Chem. Rev.* **1998**, *171*, 287–307.
- [21] P. Pertici, G. Vitulli, M. Gleria, G. Facchin, R. Milani, R. Bertani, *Macromol. Symp.* **2006**, *235*, 98–114.
- [22] H. R. Allcock, *Chemistry and applications of polyphosphazenes*, Wiley-Interscience, Hoboken, NJ, **2003**.
- [23] H. R. Allcock, *J. Inorg. Organomet. Polym. Mater.* **2007**, *17*, 349–359.
- [24] H. J. Bolink, S. G. Santamaria, S. Sudhakar, C. Zhen, A. Sellinger, *Chem. Commun.* **2008**, 618–620.
- [25] D. A. Stone, Y. Chang, H. R. Allcock, *J. Polym. Sci., Part A: Polym. Chem.* **2005**, *44*, 69–76.
- [26] S. Sudhakar, A. Sellinger, *Macromol. Rapid Commun.* **2006**, *27*, 247–254.
- [27] Y. T. Kononenko, D. Bogdal, V. M. Yashchuk, A. Burczyk, J. Pielichowski, K. M. Kushnir, *J. Mol. Liq.* **2006**, *127*, 118–120.
- [28] H. J. Bolink, E. Barea, R. D. Costa, E. Coronado, S. Sudhakar, C. Zhen, A. Sellinger, *Org. Electron.* **2008**, *9*, 155–163.
- [29] R. Horvath, C. A. Otter, K. C. Gordon, A. M. Brodie, E. W. Ainscough, *Inorg. Chem.* **2010**, *49*, 4073–4083.
- [30] F. Neve, A. Crispini, C. Di Pietro, S. Campagna, *Organometallics* **2002**, *21*, 3511–3518.
- [31] E. W. Ainscough, A. M. Brodie, G. B. Jameson, C. A. Otter, *Polyhedron* **2007**, *26*, 460–471.
- [32] H. R. Allcock, N. J. Sunderland, A. P. Primrose, A. L. Rheingold, I. A. Guzei, M. Parvez, *Chem. Mater.* **1999**, *11*, 2478–2485.
- [33] T. S. Cameron, B. Borecka, *Phosphorus Sulfur Silicon Relat. Elem.* **1992**, *64*, 121–128.
- [34] H. R. Allcock, M. L. Levin, *Macromolecules* **1985**, *18*, 1324–1330.
- [35] R. C. Haddon, S. V. Chichester-Hicks, S. L. Mayo, *Inorg. Chem.* **1988**, *27*, 1911–1915.
- [36] H. R. Allcock, *Acc. Chem. Res.* **1978**, *11*, 81–87.
- [37] E. C. Constable, R. P. G. Henney, T. A. Leese, D. A. Tocher, *J. Chem. Soc., Chem. Commun.* **1990**, 513–515.
- [38] C. J. Orme, J. R. Klaehn, F. F. Stewart, *J. Membr. Sci.* **2004**, *238*, 47–55.
- [39] G. A. Carriedo, F. J. G. Alonso, D. L. Pancorbo, *Eur. Polym. J.* **2007**, *43*, 57–64.
- [40] G. A. Carriedo, A. P. Soto, M. L. Valenzuela, M. P. Tarazona, E. Saiz, *Macromolecules* **2008**, *41*, 1881–1885.
- [41] R. Kia, H. K. Fun, *Acta Crystallogr., Sect. E: Struct. Rep. Online* **2009**, *65*, m192–m193.
- [42] J. Muthukumar, M. Kannan, A. Vanitha, B. Manimaran, R. Krishna, *Acta Crystallogr., Sect. E: Struct. Rep. Online* **2010**, *66*, m558–m559.
- [43] P. J. Walsh, K. C. Gordon, D. L. Officer, W. M. Campbell, *THEOCHEM* **2006**, *759*, 17–24.
- [44] R. Horvath, K. C. Gordon, *Coord. Chem. Rev.* **2010**, *254*, 2505–2518.
- [45] C. M. McGoverin, T. J. Walsh, K. C. Gordon, A. J. Kay, A. D. Woolhouse, *Chem. Phys. Lett.* **2007**, *443*, 298–303.
- [46] N. J. Lundin, P. J. Walsh, S. L. Howell, J. J. McGarvey, A. G. Blackman, K. C. Gordon, *Inorg. Chem.* **2005**, *44*, 3551–3560.
- [47] D. M. Cleland, G. Irwin, P. Wagner, D. L. Officer, K. C. Gordon, *Chem. Eur. J.* **2009**, *15*, 3682–3690.
- [48] P. J. Walsh, K. C. Gordon, N. J. Lundin, A. G. Blackman, *J. Phys. Chem. A* **2005**, *109*, 5933–5942.
- [49] T. M. Clarke, K. C. Gordon, D. L. Officer, S. B. Hall, G. E. Collis, A. K. Burrell, *J. Phys. Chem. A* **2003**, *107*, 11505–11516.
- [50] J. C. Earles, K. C. Gordon, D. L. Officer, P. Wagner, *J. Phys. Chem. A* **2007**, *111*, 7171–7180.
- [51] S. L. Howell, K. C. Gordon, *J. Phys. Chem. A* **2004**, *108*, 2536–2544.
- [52] K. A. Walters, Y.-J. Kim, J. T. Hupp, *Inorg. Chem.* **2002**, *41*, 2909–2919.
- [53] S.-W. Lai, M. C.-W. Chan, T.-C. Cheung, S.-M. Peng, C.-M. Che, *Inorg. Chem.* **1999**, *38*, 4046–4055.
- [54] S. W. Lai, T. C. Cheung, M. C. Chan, K. K. Cheung, S. M. Peng, C. M. Che, *Inorg. Chem.* **2000**, *39*, 255–262.
- [55] C. Cornioley-Deuschel, A. Von Zelewsky, *Inorg. Chem.* **1987**, *26*, 3354–3358.
- [56] A. Y. Hirakawa, M. Tsuboi, *Science* **1975**, *188*, 359–361.
- [57] R. J. H. Clark, T. J. Dines, *Angew. Chem. Int. Ed. Engl.* **1986**, *25*, 131–160.
- [58] R. F. Dallinger, W. H. Woodruff, *J. Am. Chem. Soc.* **1979**, *101*, 4391–4393.

- [59] K. C. Gordon, J. J. McGarvey, *Chem. Phys. Lett.* **1989**, *162*, 117–122.
- [60] Calculated by comparison of the number of photons in a pulse (5.5×10^{15} photons at 355 nm) with the number of molecules in the sample. At a spot-size of approximately 300 μm and a penetration depth of 1 mm, the irradiated volume of the sample is 2.83×10^{-7} L, which corresponds to 1.70×10^{14} molecules.
- [61] F. Neve, M. Ghedini, O. Francescangeli, S. Campagna, *Liq. Cryst.* **1998**, *24*, 673–680.
- [62] G. K. Anderson, M. Lin, *Inorg. Synth.* **1990**, *28*, 60–63.
- [63] M. S. Kharasch, R. C. Seyler, F. R. Mayo, *J. Am. Chem. Soc.* **1938**, *60*, 882–884.
- [64] H. R. Allcock, W. R. Laredo, C. R. deDenus, J. P. Taylor, *Macromolecules* **1999**, *32*, 7719–7725.
- [65] G. A. Carriedo, L. Fernandez-Catuxo, F. J. G. Alonso, P. Gomez-Elife, P. A. Gonzalez, *Macromolecules* **1996**, *29*, 5320–5325.
- [66] S. J. Lind, K. C. Gordon, M. R. Waterland, *J. Raman Spectrosc.* **2008**, *39*, 1556–1567.
- [67] *SMART and SAINT, Area Detector Control and Integration Software*, Siemens Analytical X-ray Systems Inc., Madison, WI, **1996**.
- [68] G. M. Sheldrick, *SHELXTL*, Universität Göttingen, Germany, **1998**.
- [69] P. Van der Sluis, A. L. Spek, *Acta Crystallogr., Sect. A* **1990**, *46*, 194–201.

Received: March 31, 2011
Published Online: August 2, 2011